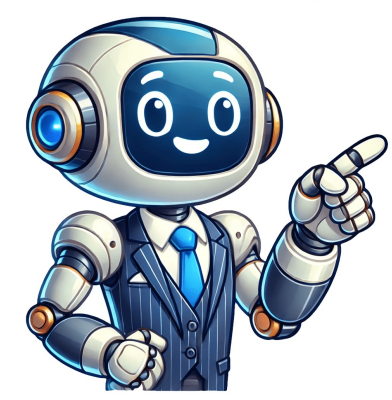


**Continue**































database retrieval system. Please enable Javascript in order to use PubChem website. Share copy and redistribute the material in any medium or format for any purpose, even commercially. Adapt, transform, and build upon the material for any purpose, even commercially. The licensor cannot revoke these freedoms as long as you follow the terms of Attribution. You must give appropriate credit, provide a link to the license, and indicate if changes were made. You may do so in any reasonable manner, but not in any way that suggests the licensor endorses you or your use. ShareAlike If you remix, transform, or build upon the material, you must distribute your contributions under the same license as the original. No additional restrictions You may not apply legal terms or technological measures that legally restrict others from doing anything the license permits. You do not have to comply with the license for elements of the material in the public domain or where your use is permitted by an applicable exception or limitation. No warranties are given. The license may not give you all of the permissions necessary for your intended use. For example, other rights such as publicity, privacy, or moral rights may limit how you use the material. As a library, NLM provides access to scientific literature. Inclusion in an NLM database does not imply endorsement of, or agreement with, the contents by NLM or the National Institutes of Health. Learn more: PMC Disclaimer | PMC Copyright Notice. 2022 Apr 15;27(8):2557. doi: 10.3390/molecules27082557. Metakaolin-based geopolymers microspheres (NMGM) with hierarchical pore structures were prepared by suspension dispersion method in dimethyl sulfoxide at 80 °C. The hydrothermal modification of NMGM was carried out at a lower temperature of 80 °C, and NaA molecular sieve converted from metakaolin-based geopolymers (NMGM) with good crystal structure was prepared and applied in thermal catalytic cracking of low-density polyethylene (LDPE) reaction. The one-pot two-stage thermal catalytic cracking of waste LDPE was carried out in a 100 mL micro-autoclave under normal pressure. In this work, the optimal proportions and optimal reaction conditions of catalysts for NMGM thermal catalytic cracking of LDPE waste to fuel oil were investigated. The NMGM catalyst showed high selectivity to the liquid product of thermal catalytic cracking of waste LDPE. Under the reaction conditions of reaction time of 1 h and reaction temperature of 400 °C, the liquid-phase yield of thermal catalytic cracking of LDPE reached a high of 88.45%, of which the content of gasoline components was 10.14% and the content of diesel components was 80.97%. Keywords: geopolymers, NaA molecular sieve, catalysts, plastic waste, fuel oil. Plastics are durable and cheap, so they have become a common item in thousands of households, which greatly facilitates human life. It was once hailed as one of the greatest inventions of the 20th century. Over time, plastic has gone from a lauded invention to one of the biggest enemies of environmental pollution. Although the pace of technological development continues to advance, the problem of plastic pollution has not yet been fundamentally solved. Microplastics, which have been widely criticized in recent years, refer to plastic particles smaller than 5 mm that cannot be degraded in a short period of time and thus remain in the environment, and are difficult to be detected by the naked eye [1,2]. Microplastics have been detected in the sparsely populated Arctic [3,4]. Microplastics enter the diet of marine organisms, accumulate in the biological chain, and then enter the human table, endangering human health [5]. Landfilling plastics in traditional plastic-disposal methods will bring about secondary pollution problems. Plastics have a high calorific value (CV) that matches conventional fuels such as gasoline, kerosene, diesel, etc., so incinerating plastics to generate electricity, steam and heat is also a major way of recycling. However, its economic value has been questioned and the emission of toxic pollutants such as dioxins and furans have not been resolved [6,7]. The above two methods will bring about the problem of secondary pollution, but most developing countries are still using these two types of traditional treatment solutions [8]. At present, researchers focus on two solutions to plastic pollution: one is research on degradable plastics, and the other is research on cracking plastics to high-value-added products [9,10,11,12]. The research and development of degradable plastics is considered to solve the problem of plastic pollution from the root cause, but degradable plastics are still inferior to traditional plastics in terms of finished-product quality and performance. Degradable plastics have a large gap compared with traditional plastics, with good tensile strength and elongation at break, and the cost is much higher than traditional plastics [13]. As a degradable plastic as a packaging material, its biodegradability needs to be improved, and it cannot degrade quickly and completely after completing the mission of packaging, and the residue is difficult to degrade, causing land pollution [14]. Therefore, there are a series of scientific and technological problems in the process of optimizing the performance of degradable plastics. It is currently popular to recycle plastics into gaseous and liquid products with high added value [15,16,17]. Methods of gasifying plastic waste into syngas have been studied, but their recycling is expensive [18]. Cracking plastic wastes into fuel (gasoline, diesel) is convenient for transportation and has practical significance in rapidly rising oil prices. The cracking method can be divided into pyrolysis, catalytic cracking, and a method combining pyrolysis and catalytic cracking [19]. The pyrolysis reaction needs to be carried out at a high temperature of 500 to 900 °C; the operating temperature is high, and the heat demand increases sharply because the pyrolysis is an endothermic reaction [20]. The carbon-number distribution of the product after pyrolysis is wide, and further processing is required to improve the quality of the oil in the product. The catalytic-cracking method uses a catalyst, which can reduce the activation energy required for the reaction, so that the plastic is cracked at a lower reaction temperature [21]. The use of suitable catalysts can narrow the distribution of reaction products, improve the selectivity of target products, and reduce subsequent separation and processing procedures. The combined method of thermal cracking and catalytic cracking can be divided into catalytic pyrolysis, thermal cracking-catalytic cracking, and catalytic cracking-catalytic upgrading [22]. The catalyst in the catalytic-pyrolysis process is mixed with a plastic sample in a batch reactor. The disadvantage of this process is the high tendency to form coke on the catalyst surface, which reduces catalyst efficiency over time and results in high residue yields. In addition to this, the separation of the residue from the catalyst at the end of the experiment was difficult. Catalytic cracking-catalytic upgrading means adding a small amount of catalyst in the pyrolysis stage of the two-step method, thereby shortening the cracking time and reducing the cracking temperature [23]. However, its shortcomings are also more obvious, and there is no economic benefit. The difference between the thermal cracking-catalytic cracking upgrading conversion method and the catalytic cracking-catalytic upgrading conversion method is that there is no catalyst involved in the thermal cracking process [24]. Molten plastics have high viscosity and low thermal conductivity, which will cause a series of heat- and mass-transfer problems. Therefore, many scholars have carried out research on the selection of plastic-cracking reactors, so as to improve the mass transfer and heat transfer of the reaction process. Kaminsky et al. [25] developed a process consisting mainly of a fluidized-bed reactor, ensuring a uniform temperature throughout the reactor. Fluidized beds can be operated with a continuous plastic feed, which is beneficial for scaling up the process, but when operating conditions are out of range, molten plastic-coated particles can agglomerate and bed deflow occurs [26]. The helical kiln consists of a tubular reactor and a screw conveyor. The residence time of the polymer can be controlled by changing the speed of the screw, and the heat-transfer rate and pyrolysis temperature can be well-controlled [27]. The gas-solid contact in the spouted-bed reactor is violent, and it can be used to treat irregular particles, fine particles, and other materials that are difficult to deal with by other methods of gas-solid contact [28]. Fixed-bed reactors are usually operated in batch mode during the pyrolysis of waste plastics [29]. Due to the poor heat- and mass-transfer efficiency of the molten plastic, the pyrolysis products initially formed from the plastic in the fixed-bed reactor are usually passed into another reactor for further cracking under the purging of an inert gas stream. Because batch or semi-batch reactor parameters are easy to control, they are the best reactors for obtaining high liquid yields, and their main disadvantage is the tendency to form coke on the outer surface of the catalyst, thereby reducing the overall yield of liquid product [30]. In this work, the method of separating the catalyst from the cracking raw materials is adopted, and the low-density polyethylene at the bottom is heated to vaporize it through the catalyst in the pyrolysis layer, and the thermal cracking and catalytic cracking are combined. A one-pot two-stage reaction. Compared with the traditional thermal cracking-catalytic upgrading method, this method is more convenient and saves on equipment and equipment cost. This is referred to herein simply as thermal catalytic cracking. The key to the thermal catalytic cracking-catalytic upgrading process is the catalyst. Due to the high activity of solid acid catalysts in the cracking of plastic wastes into oil, researchers are currently focusing on this type of catalysts [31,32]. However, its high-strength acidity can easily lead to the deactivation of the catalyst. Zeolite molecular sieves with high Si/Al ratio, such as ZSM-5 [33,34], HZSM-5 [24] and H [35], are all high-strength acid catalysts, which are expensive to prepare and require high-precision preparation technology. The degradation effect of different catalysts on plastics has been investigated by many researchers and examined using kinetic parameters determined by different models. Khan et al. [36] used a commercial LZ-Y52 molecular-sieve catalyst to react at 370 °C for 60 min, and the oil yield exceeded 40%. Nisar et al. [37] calculated the kinetic parameters and found that the use of catalysts can reduce the activation energy of the reaction. Aguado et al. [38] found that mesoporous catalysts with high accessibility of plastic molecules and catalysts with small crystal size (high specific surface area) are expected to improve the catalytic activity of plastic cracking. Geopolymer is a three-dimensional network gel with amorphous and quasi-crystalline characteristics, which is formed by the polymerization of silicon-oxygen tetrahedron and aluminum-oxygen tetrahedron, which is similar to zeolite in chemical composition [39,40,41]. The production-energy consumption of geopolymers is low, equivalent to only 30% of the energy consumption of cement production. Geopolymer properties and formation methods are similar to natural zeolites. The zeolite molecular-sieve microspheres prepared from geopolymers have suitable acidity and controllable acidity. Microspheres with a hierarchical pore structure can be prepared by adding a suitable foaming agent, which provides abundant acidic reaction sites and channels for the catalytic cracking of plastics [42]. Alkali-excited geopolymers have high mechanical strength, so recovery after the reaction is complete is convenient. At present, commercial catalysts still have problems such as low selectivity of oil products and low quality of oil products, high cost of catalyst preparation and easy deactivation, and high energy consumption caused by high cracking temperature. The problem of environmental pollution caused by plastics is becoming more and more serious, and the price of oil and oil is rising. Therefore, it is of practical significance to develop an inexpensive plastic-cracking catalyst with high selectivity. In this work, metakaolin was used as raw material, sodium hydroxide was used as alkali activator, and 0.1wt% H2O2 and 0.05wt% K12 were added to prepare geopolymers with hierarchical pore structure and low Si/Al ratio. It was hydrothermally treated and successfully converted into a metakaolin-NaA molecular sieve (NMGM), which was used in the thermal catalytic cracking of urban solid plastic LDPE to make fuel oil. The changes of NMGM catalyst-preparation conditions and reaction conditions on the yield and hydrocarbon composition of liquid-phase products from thermal catalytic cracking of waste LDPE were investigated. The Na2O/SiO2 of the catalyst was varied by varying the amount of NaOH added during the preparation of the NMGM catalyst. The prepared microspheres were all hydrothermally treated at 80 °C for 1 d. From the SEM test at 100 m, the microspheres remained spherical after hydrothermal treatment (Figure 1b,d,f,h). When Na2O/SiO2 was 0.2, the molecular-sieve grains obtained by the transformation of geopolymers could not be found (Figure 1a). When the dosage of NaOH was increased to Na2O/SiO2 of 0.4, a few polyhedral grains with a diameter of about 1 m were observed on the surface of the microspheres (Figure 1c). When the Na2O/SiO2 ratio was 0.8, a large number of cubic molecular-sieve grains with side lengths of about 0.68 m were formed on the surface of the microspheres, and many macropores could be observed on the surface (Figure 1e). When Na2O/SiO2 was 0.2, the amount of alkali activator reached its peak, and the surface of the microspheres was denser than the first three groups. It could be observed that the molecular sieves have different grain sizes and rough edges (Figure 1g). SEM and XRD tests of NMGM with different NaOH additions: (a,c,e,g) are the SEM tests of NMGM with Na2O/SiO2 of 0.2, 0.4, 0.8, 1.2, respectively; (b,d,f,h) SEM of NMGM with Na2O/SiO2 of 0.2, 0.4, 0.8, 1.2, respectively; (i) is the XRD pattern of different Na2O/SiO2 ratios (\*: characteristic peaks of NaA molecular sieves). From Figure 1i, there were ten main characteristic peaks in the standard card spectrum of the NaA molecular sieve. The 2 of ten main characteristic peaks were the diffraction peaks at 7.18, 10.16, 12.45, 21.65, 23.96, 26.09, 27.09, 29.92, and 34.17, respectively. With the increase in alkali activator, the crystallinity of NMGM first increased and then decreased. The NaA molecular sieve with higher crystallinity could be obtained by adding an appropriate amount of NaOH. When the amount of alkali activator was insufficient, the metakaolin could not be fully excited, and it mainly presented an amorphous dispersion peak between 20 and 30 of 2. If the alkali activator was used in excess, the formed NaA molecular-sieve crystal could not be fully excited, and it mainly presented an amorphous dispersion peak between 20 and 30 of 2. The alkali activator was used in excess, due to the influence of the high-alkaline environment, the formed NaA molecular-sieve crystal grained with complete crystal form would be dissolved again [43]. In this work, a Na2O/SiO2 ratio of 0.8 was chosen as the base activator dosage for the preparation of NMGM catalysts. The XRD test showed that the crystallinity of metakaolin-based geopolymers converted into NaA molecular sieve was affected by hydrothermal time. When the hydrothermal time was 1 d, the diffraction peaks would be transformed from the initial amorphous diffraction peaks to the crystalline diffraction peaks of NaA molecular sieves. Among them, when the hydrothermal time was 2 d, the diffraction peak intensity was the strongest, and the crystallinity was the highest. When the hydrothermal time was extended to 3 d, the intensity of diffraction peaks decreased instead (Figure 2a). The in situ transformation of geopolymers into molecular sieves could be divided into nucleation and growth stages. The alkalinity in the hydrothermal solvent reached the maximum when the conversion rate of molecular sieves reached the maximum. At this time, if the hydrothermal treatment was not stopped, part of the formed molecular sieve would dissolve and collapse. Therefore, the long-term hydrothermal treatment would cause the intensity of the diffraction peak to weaken. XRD test and BET test of NMGM catalyst with Na2O/SiO2 of 0.8 at hydrothermal time of 0 d, 1 d, 2 d, 3 d: (a) XRD (\*: characteristic peaks of NaA molecular sieves), (b) pore-size distribution, (c) specific surface area. The BET test of the microspheres subjected to different hydrothermal times clearly showed that the NMGM catalyst was a porous structure dominated by mesopores and macropores from the pore-size distribution map (Figure 2b). The presence of catalyst mesopores plays a positive role in plastic cracking, and Sakata et al. [44] claim that KFS-16 is a pure silica mesoporous material without acid sites. However, it can crack polyethylene as quickly as silica-alumina, thereby producing more liquid. This is because mesopores act as sites for long-term storage of free-radical species, so abundant free radicals may accelerate plastic degradation. When the hydrothermal time was 1 d, the specific surface area of NMGM reached the maximum, which was 38.49 m<sup>2</sup>/g (Figure 2c). At this time, the NaA molecular sieve had experienced a period of growth, and the larger NaA molecular-sieve crystals grew in a staggered manner, resulting in numerous pores. The hydrothermal time continued to extend to 2 d, and the specific surface area decreased to 23.11 m<sup>2</sup>/g. At this time, the growth of NaA molecular-sieve crystals reached saturation, and the formation of excessive molecular-sieve crystals blocked some of the pores, resulting in a decrease in the specific surface area. When the hydrothermal time was 3 d, some of the formed NaA molecular-sieve grains were dissolved and collapsed under strong alkaline conditions, resulting in blockage and collapse of some of the pores of NMGM, and the specific surface area and pore size were reduced. The increase in specific surface area and the existence of mesopores had a positive effect on the thermal catalytic cracking of LDPE. The NMGM catalyst prepared in this work selects 1 d as the optimal hydrothermal modification time for the conversion of metakaolin-based geopolymers into NaA molecular sieves. NH3-TPD tests were performed on NMGM that were not hydrothermally and hydrothermally modified for 1 d at 80 °C (Figure 3). The changes in acid properties of NMGM after hydrothermal modification were significant, and the total acid content increased from 45.01 mol/g to 95.01 mol/g. The total acid content and pore structure of the catalyst determine its catalytic activity in acid-catalyzed reactions [31]. After hydrothermal treatment for 1 d, the NMGM catalyst was converted from an amorphous structure to a NaA molecular sieve, resulting in a significant increase in the total acid content and abundant pores, thereby improving the reactivity of the catalyst. The total acid content of the catalyst was related to the specific surface area of the catalyst and the density of acid sites on the catalyst surface. NH3-TPD tests of NMGM before and after hydrothermal 1 d. After hydrothermal treatment for 1 d, NMGM had three desorption peaks: the low-temperature peak corresponded to the weak acid site, the high-temperature peak corresponded to the strong-acid site, and the middle peak was the medium strong-acid site. After hydrothermal modification, the strong-acid center of NMGM did not shift greatly compared with that before hydrothermal modification, and the overall acidic reaction site was composed of weak acid and medium strong acid, which is a catalyst of non-high-strength acid type. Sakata et al. [44] explored the effect of catalyst acidity on the distribution of HDPE pyrolysis products. The results of the acidity-strength test of the catalyst showed that SA-1 > ZSM-5 > SA-2. The results showed that SA-2 catalyst with lower acidity was observed to produce the highest amount of liquid oil, and ZSM-5 with strong-acid sites tended to produce more gaseous products with very low liquid yield. Appropriate acidity is beneficial to inhibit excessive cracking of liquid products and prepare liquid products with high selectivity. The molten LDPE was directly mixed with the catalyst, it would easily adhere to the surface and block the catalyst pores, increasing the occurrence of coking reaction. In this experiment, the solid-plastic waste LDPE raw materials were first pyrolyzed and vaporized at the bottom of the quartz cup glass, and then catalytically cracked with the NMGM catalyst on the upper layer of quartz wool under the purging of N<sub>2</sub>. Used NMGM before and after hydrothermal modification at 80 °C for 1 d, the results of catalytic thermal cracking of waste LDPE at 400 °C for 1 h are shown in Figure 4. The yield of liquid oil in the cracked product increased from 23.51 wt% to 68.45 wt%, and the solid yield decreased from 38.59 wt% to 34.86 wt% (Figure 4a). The yield of aromatic products in the liquid fraction increased from 1.18% to 6.79%. After hydrothermal treatment, the content of hydroxyl groups in the pores of the NMGM microspheres and on the surface of the microspheres decreased, so the hydroxyl groups involved in the replacement reaction decreased, and the yield of alcohol products decreased significantly, from 47.88% to 20.33% (Figure 4b). Product test of NMGM before and after hydrothermal treatment. The stretching vibration peaks of the C-H bond at 2925.51 cm<sup>-1</sup> and the shear and bending vibration peaks of the C-H bond at 1469.87 cm<sup>-1</sup> confirmed the existence of alkanes in the liquid product, and their peak intensity was enhanced. In the infrared test results of the liquid-phase product after hydrothermal NMGM-cracking waste LDPE, the strength of the stretching vibration peak of the C=O bond at 1639.46 cm<sup>-1</sup> and the C-H bending vibration peak at 967.74 cm<sup>-1</sup> of the olefin were weakened. The appearance of the C-H bending vibration peak at 721.69 cm<sup>-1</sup> indicates the presence of olefinic and aromatic compounds in the product. Figure 5 shows the reaction time of 1 h at 350 °C, 400 °C and 450 °C in a 100 mL micro-autoclave reactor system with a feed/catalyst ratio of 5, the activity test results of NMGM catalyst for thermal catalytic cracking of LDPE plastic into fuel oil. Product tests after thermal catalytic cracking of waste LDPE at 350 °C, the specific surface area of NMGM reached the maximum, which was 38.49 m<sup>2</sup>/g (Figure 2c). At this time, the NaA molecular sieve had experienced a period of growth, and the larger NaA molecular-sieve crystals grew in a staggered manner, resulting in numerous pores. The hydrothermal time continued to extend to 2 d, and the specific surface area decreased to 23.11 m<sup>2</sup>/g. At this time, the growth of NaA molecular-sieve crystals reached saturation, and the formation of excessive molecular-sieve crystals blocked some of the pores, resulting in a decrease in the specific surface area. When the hydrothermal time was 3 d, some of the formed NaA molecular-sieve grains were dissolved and collapsed under strong alkaline conditions, resulting in blockage and collapse of some of the pores of NMGM, and the specific surface area and pore size were reduced. The increase in specific surface area and the existence of mesopores had a positive effect on the thermal catalytic cracking of LDPE. The NMGM catalyst prepared in this work selects 1 d as the optimal hydrothermal modification time for the conversion of metakaolin-based geopolymers into NaA molecular sieves. NH3-TPD tests were performed on NMGM that were not hydrothermally and hydrothermally modified for 1 d at 80 °C (Figure 3). The changes in acid properties of NMGM after hydrothermal modification were significant, and the total acid content increased from 45.01 mol/g to 95.01 mol/g. The total acid content and pore structure of the catalyst determine its catalytic activity in acid-catalyzed reactions [31]. After hydrothermal treatment for 1 d, the NMGM catalyst was converted from an amorphous structure to a NaA molecular sieve, resulting in a significant increase in the total acid content and abundant pores, thereby improving the reactivity of the catalyst. The total acid content of the catalyst was related to the specific surface area of the catalyst and the density of acid sites on the catalyst surface. NH3-TPD tests of NMGM before and after hydrothermal 1 d. After hydrothermal treatment for 1 d, NMGM had three desorption peaks: the low-temperature peak corresponded to the weak acid site, the high-temperature peak corresponded to the strong-acid site, and the middle peak was the medium strong-acid site. After hydrothermal modification, the strong-acid center of NMGM did not shift greatly compared with that before hydrothermal modification, and the overall acidic reaction site was composed of weak acid and medium strong acid, which is a catalyst of non-high-strength acid type. Sakata et al. [44] explored the effect of catalyst acidity on the distribution of HDPE pyrolysis products. The results of the acidity-strength test of the catalyst showed that SA-1 > ZSM-5 > SA-2. The results showed that SA-2 catalyst with lower acidity was observed to produce the highest amount of liquid oil, and ZSM-5 with strong-acid sites tended to produce more gaseous products with very low liquid yield. Appropriate acidity is beneficial to inhibit excessive cracking of liquid products and prepare liquid products with high selectivity. The molten LDPE was directly mixed with the catalyst, it would easily adhere to the surface and block the catalyst pores, increasing the occurrence of coking reaction. In this experiment, the solid-plastic waste LDPE raw materials were first pyrolyzed and vaporized at the bottom of the quartz cup glass, and then catalytically cracked with the NMGM catalyst on the upper layer of quartz wool under the purging of N<sub>2</sub>. Used NMGM before and after hydrothermal modification at 80 °C for 1 d, the results of catalytic thermal cracking of waste LDPE at 400 °C for 1 h are shown in Figure 4. The yield of liquid oil in the cracked product increased from 23.51 wt% to 68.45 wt%, and the solid yield decreased from 38.59 wt% to 34.86 wt% (Figure 4a). The yield of aromatic products in the liquid fraction increased from 1.18% to 6.79%. After hydrothermal treatment, the content of hydroxyl groups in the pores of the NMGM microspheres and on the surface of the microspheres decreased, so the hydroxyl groups involved in the replacement reaction decreased, and the yield of alcohol products decreased significantly, from 47.88% to 20.33% (Figure 4b). Product test of NMGM before and after hydrothermal treatment. The stretching vibration peaks of the C-H bond at 2925.51 cm<sup>-1</sup> and the shear and bending vibration peaks of the C-H bond at 1469.87 cm<sup>-1</sup> confirmed the existence of alkanes in the liquid product, and their peak intensity was enhanced. In the infrared test results of the liquid-phase product after hydrothermal NMGM-cracking waste LDPE, the strength of the stretching vibration peak of the C=O bond at 1639.46 cm<sup>-1</sup> and the C-H bending vibration peak at 967.74 cm<sup>-1</sup> of the olefin were weakened. The appearance of the C-H bending vibration peak at 721.69 cm<sup>-1</sup> indicates the presence of olefinic and aromatic compounds in the product. Figure 5 shows the reaction time of 1 h at 350 °C, 400 °C and 450 °C in a 100 mL micro-autoclave reactor system with a feed/catalyst ratio of 5, the activity test results of NMGM catalyst for thermal catalytic cracking of LDPE plastic into fuel oil. Product tests after thermal catalytic cracking of waste LDPE at 350 °C, the specific surface area of NMGM reached the maximum, which was 38.49 m<sup>2</sup>/g (Figure 2c). At this time, the NaA molecular sieve had experienced a period of growth, and the larger NaA molecular-sieve crystals grew in a staggered manner, resulting in numerous pores. The hydrothermal time continued to extend to 2 d, and the specific surface area decreased to 23.11 m<sup>2</sup>/g. At this time, the growth of NaA molecular-sieve crystals reached saturation, and the formation of excessive molecular-sieve crystals blocked some of the pores, resulting in a decrease in the specific surface area. When the hydrothermal time was 3 d, some of the formed NaA molecular-sieve grains were dissolved and collapsed under strong alkaline conditions, resulting in blockage and collapse of some of the pores of NMGM, and the specific surface area and pore size were reduced. The increase in specific surface area and the existence of mesopores had a positive effect on the thermal catalytic cracking of LDPE. The NMGM catalyst prepared in this work selects 1 d as the optimal hydrothermal modification time for the conversion of metakaolin-based geopolymers into NaA molecular sieves. NH3-TPD tests were performed on NMGM that were not hydrothermally and hydrothermally modified for 1 d at 80 °C (Figure 3). The changes in acid properties of NMGM after hydrothermal modification were significant, and the total acid content increased from 45.01 mol/g to 95.01 mol/g. The total acid content and pore structure of the catalyst determine its catalytic activity in acid-catalyzed reactions [31]. After hydrothermal treatment for 1 d, the NMGM catalyst was converted from an amorphous structure to a NaA molecular sieve, resulting in a significant increase in the total acid content and abundant pores, thereby improving the reactivity of the catalyst. The total acid content of the catalyst was related to the specific surface area of the catalyst and the density of acid sites on the catalyst surface. NH3-TPD tests of NMGM before and after hydrothermal 1 d. After hydrothermal treatment for 1 d, NMGM had three desorption peaks: the low-temperature peak corresponded to the weak acid site, the high-temperature peak corresponded to the strong-acid site, and the middle peak was the medium strong-acid site. After hydrothermal modification, the strong-acid center of NMGM did not shift greatly compared with that before hydrothermal modification, and the overall acidic reaction site was composed of weak acid and medium strong acid, which is a catalyst of non-high-strength acid type. Sakata et al. [44] explored the effect of catalyst acidity on the distribution of HDPE pyrolysis products. The results of the acidity-strength test of the catalyst showed that SA-1 > ZSM-5 > SA-2. The results showed that SA-2 catalyst with lower acidity was observed to produce the highest amount of liquid oil, and ZSM-5 with strong-acid sites tended to produce more gaseous products with very low liquid yield. Appropriate acidity is beneficial to inhibit excessive cracking of liquid products and prepare liquid products with high selectivity. The molten LDPE was directly mixed with the catalyst, it would easily adhere to the surface and block the catalyst pores, increasing the occurrence of coking reaction. In this experiment, the solid-plastic waste LDPE raw materials were first pyrolyzed and vaporized at the bottom of the quartz cup glass, and then catalytically cracked with the NMGM catalyst on the upper layer of quartz wool under the purging of N<sub>2</sub>. Used NMGM before and after hydrothermal modification at 80 °C for 1 d, the results of catalytic thermal cracking of waste LDPE at 400 °C for 1 h are shown in Figure 4. The yield of liquid oil in the cracked product increased from 23.51 wt% to 68.45 wt%, and the solid yield decreased from 38.59 wt% to 34.86 wt% (Figure 4a). The yield of aromatic products in the liquid fraction increased from 1.18% to 6.79%. After hydrothermal treatment, the content of hydroxyl groups in the pores of the NMGM microspheres and on the surface of the microspheres decreased, so the hydroxyl groups involved in the replacement reaction decreased, and the yield of alcohol products decreased significantly, from 47.88% to 20.33% (Figure 4b). Product test of NMGM before and after hydrothermal treatment. The stretching vibration peaks of the C-H bond at 2925.51 cm<sup>-1</sup> and the shear and bending vibration peaks of the C-H bond at 1469.87 cm<sup>-1</sup> confirmed the existence of alkanes in the liquid product, and their peak intensity was enhanced. In the infrared test results of the liquid-phase product after hydrothermal NMGM-cracking waste LDPE, the strength of the stretching vibration peak of the C=O bond at 1639.46 cm<sup>-1</sup> and the C-H bending vibration peak at 967.74 cm<sup>-1</sup> of the olefin were weakened. The appearance of the C-H bending vibration peak at 721.69 cm<sup>-1</sup> indicates the presence of olefinic and aromatic compounds in the product. Figure 5 shows the reaction time of 1 h at 350 °C, 400 °C and 450 °C in a 100 mL micro-autoclave reactor system with a feed/catalyst ratio of 5, the activity test results of NMGM catalyst for thermal catalytic cracking of LDPE plastic into fuel oil.

evaluated various zeolite catalysts at 330C, achieving acceptably high conversion and high liquid selectivity, highlighting disparities among samples. The use of zeolites greatly enhances the conversion of PE at low temperatures by accelerating C-C bond scission, catalyzed by Brønsted acid sites that promote the carbonium or carbonium mechanisms<sup>28</sup>. In absence of zeolites, just a 0.2 % PE conversion was observed at 330C. To evaluate the effect of zeolite topologies, several commercially available zeolites, including ZSM-5 (MFI), zeolite beta (\*BEA), and zeolite Y (FAU) were examined (Supplementary Fig.5). These zeolites achieved PE conversions ranging from 20% to 80% at the same temperature. Details on the tested commercial zeolites are provided in the Supplementary Figs.1, 2 and Supplementary Table1. All zeolites demonstrated notable isomerization, as indicated by the complexity of the resulting gas chromatograph (GC) profiles (see Supplementary Figs.6, 7). Among the tested commercial zeolites, ZSM-5 having micropores limited to 10MR pore openings, exhibited the highest conversion, but its liquid selectivity was lower than that of zeolite beta due to its high gas selectivity as depicted in Fig.2e, which originated from its narrow pore system. ZSM-5 also tended to produce lighter liquid products than the other two frameworks (Fig.2f). The 1H and 13C NMR spectra for the same liquid product mixtures are also presented in Supplementary Fig.8. The 1H NMR spectra indicate that the products contain the most olefinic sp<sup>2</sup> C-H in the order of ZSM-5>zeolite beta>zeolite Y. This matches the order of PE conversion (Fig.2e), presumably due to the high frequency of chain scission via the -scission occurred over ZSM-5.

Conversely, the lowest PE conversion and olefinic proton content observed in the zeolite Y samples are likely due to their relatively weak acid sites<sup>41</sup>. The zeolite beta sample of 12MR pore openings achieved a PE conversion comparable to ZSM-5 with the highest liquid selectivity. In this work, the effects of the intrinsic properties of zeolite on the catalytic cracking of LDPE\*BEA-type zeolites can be crystallized with a wide synthetic window of hydrothermal synthesis using tetraethylammonium hydroxide (TEAOH) as the organic structure-directing agent (OSDA)<sup>35</sup>. It has been observed that the crystal size of the resulting \*BEA-type zeolite crystals is strongly correlated with the Al content in the hydrothermal \*BEA-crystallizing systems<sup>35</sup>. As the Si/Al ratio of the system increases, the crystal size also increases, thereby reducing the relative contribution of acid sites on external surfaces compared to those within micropores. To decouple the Si/Al ratio from the crystal size, we employed three different hydrothermal methods from the literature and modified them to prepare three series of \*BEA-type zeolites, denoted as L-, M-, and S-series. For the preparation of large crystals (L-series, 0.651.7m), fluoride was used as the mineralizer, known to stabilize small composite building units of the \*BEA framework<sup>42,44</sup>. The medium- and small-sized \*BEA-type zeolites (M- and S-series, 130170nm and 30140nm, respectively) were obtained using conventional hydroxide media<sup>36,43</sup>. The S-series were synthesized at a low crystallization temperature of 100C, much below the conventional temperature (140C) for \*BEA synthesis. As noted above, trends observed here indicate that reducing the Al content generally led to larger crystal sizes (Fig.3a). The scanning electron micrographs (SEM) of three representative samples from the three series are shown in Fig.3b. In this work, samples are denoted as X-BEA-y, where X represents the series code (L, M, or S) and y indicates the approximate Si/Al ratio of the zeolites, as characterized by the energy dispersive spectroscopy (EDS). The sample information is summarized in Table1. Their synthetic details and additional characterization results are provided in the Supplementary Table2 and Supplementary Figs.912. Fig. 3: Relation between the Al content and crystal size of the resulting \*BEA-type zeolite. a Schematic summary of intrinsic properties-controlled beta zeolite, scanning electron microscope images of synthesized beta zeolite with Si/Al 10: b L-BEA-10, c M-BEA-10, and d S-BEA-10. Each data was provided with an error bar which was calculated via standard deviation of 10 parallel data. Large, Medium, Small crystal sized zeolite beta with y (Si/Al) denoted as L-, M-, S-BEA-y. Table 1 Physical properties of the intrinsic properties-controlled beta zeolites. The catalytic cracking of PE using the prepared \*BEA-type zeolites was tested in an open-batch configuration under optimal conditions (10mL N2/min, 330C, 2h) as previously discussed. Figure4ac show the conversion and liquid selectivity, achieved with the \*BEA-type zeolites listed in Table1. The justification for comparing the cracking behavior of zeolite beta sample series synthesized through different methods is supported by the independent 1,3,5-triisopropylbenzene (TIPB) cracking results provided in Supplementary Fig.14. The framework Al sites primarily act as Brønsted acid sites in zeolites, serving as active sites for the catalytic cracking of long-chain hydrocarbons<sup>28</sup>. Thus, the decrease in Si/Al ratios led to an increase in the PE conversion across all sample series, indicating enhanced apparent catalytic activity. Crystal size also played a crucial role in the PE conversion. The S-series samples, with higher specific external surface area values (Table1), showed higher PE conversions than the L-series samples. A similar trend was observed in liquid selectivity (Fig.4b). Al sites can be located within either the micropores or external surfaces of the zeolite samples. The catalytic conversion of PE over \*BEA-type zeolites may occur in two steps: bulky molecule scission at the external surface acid sites, followed by additional scission of smaller molecules within the micropores. We think that the molecular weight distribution of liquid products primarily depends on the spatial distributions of these acid sites as shown in Fig.4e. The S-BEA-10 sample having the most Al sites and the highest external surface area showed a high PE conversion (~80%) and liquid selectivity (~70%) at a low temperature of 330C. This result offers experimental evidence that reducing crystal size also meaningfully enhances the PE conversion and liquid selectivity by facilitating the external scission process of polymer chains. Moreover, the increase in mesopore volume associated with decreasing crystal size suggests an improvement in mass transfer efficiency, which may contribute to the observed enhancement in catalytic performance. Further analysis on the conversion and liquid selectivity is provided in the Supplementary Figs.1321. Fig. 4: Intrinsic properties-controlled beta zeolite catalytic cracking of low-density polyethylene (LDPE) at 330C, 2h, 10mL N2/min. a Conversion, b liquid selectivity, c liquid selectivity by conversion, d hydrocarbon distribution in liquid products, and e schematic description for the relation between acid site distribution and liquid product molecular weight. Large, Medium, Small crystal sized zeolite beta with y (Si/Al) denoted as L-, M-, S-BEA-y. The simulated distillation (SIMDIS) results confirmed that over 99% of the liquid portion comprises hydrocarbons in the range from C5 to C30 (Supplementary Figs.22, 23 and Table3). Figure4d illustrates the hydrocarbon distribution in liquid products from the catalytic cracking of PE over L-BEA-10, M-BEA-10, and S-BEA-10, which have similar Si/Al ratios but vary in crystal sizes. L-BEA-10 and M-BEA-10 predominantly yielded hydrocarbons in the gasoline (C510) range, whereas S-BEA-10 yielded heavier products under the same reaction conditions. Considering the total number of Al sites is similar across the three samples, it suggests that L-BEA-10 and M-BEA-10 have more micropore Al sites than S-BEA-10, providing a greater extent of secondary scission to lighter products. This serves as an example of the reactant shape selectivity. The spent catalysts were recovered as entangled chunks mixed with residues, including deposited coke species. The SIMDIS analysis of the Soxhlet extract, using toluene as the solvent, revealed a minimal composition of remaining product-range (C5C30) hydrocarbons in the solid phase (Supplementary Fig.15 and Table3). The spent catalysts should be recoverable and reusable from the remaining solid phase. However, mechanical separation of inorganic catalyst components from the mixture was unsuccessful due to the polymeric organic components remaining in the solid phase, showing a sturdy texture at room temperature. To assess catalyst reusability, a new PE feed of the same amount was directly added to the spent mixture for a second run. The conversion and liquid selectivity in the second run decreased compared to the first, from 78% to 67% and from 68% to 54%, respectively (Fig.5a). However, the product distribution of the liquid product within the range from C5 to C15 remained almost unchanged, as shown in Fig.5b, indicating that coke-induced deactivation primarily influenced the external surfaces of zeolite rather than the micropores. The zeolite catalysts could be separated by removing the residue through air calcination at 580C for 6h. The regenerated catalyst was found to have physical properties very similar to those of the virgin catalyst, as confirmed by PXRD, SEM, EDS, and BET analyses (Supplementary Fig.24). Consequently, in the catalytic cracking of PE using the regenerated catalyst, both the conversion and liquid selectivity were almost identical (Fig.5c, d). Finally, the optimized 330C open-batch reaction conditions were applied to an actual post-consumer PE waste sample collected from a local recycling center, and it was compared to two model virgin PEs with different molecular weights (4kDa and 204kDa), confirming that the resulting PE conversion and liquid selectivity were similar to those observed with the virgin PE model feed with heavier molecular weight, as illustrated in Supplementary Fig.25. Fig. 5: Catalytic cracking to evaluate reusability and regenerability of deactivated zeolite beta (S-BEA-10) at 330C, 2h, 10mL N2/min. Continuous secondary reaction compared to the first reaction. a Conversion and liquid selectivity, b hydrocarbon distribution in liquid products; show the regenerated zeolite beta catalytic cracking compared to the virgin zeolite beta, namely c conversion, d hydrocarbon distribution in liquid products. Small crystal sized zeolite beta with y (Si/Al) denoted as S-BEA-y. Conventionally, the catalytic cracking of polyolefins using zeolite catalysts have adopted operation temperatures higher than 380C (Supplementary Fig.26)<sup>33,45,46</sup>. This work demonstrates the temperature can be greatly reduced to 330C while maintaining high PE conversion and liquid selectivity, provided the reactor configuration and catalysts are adequately optimized. The open-batch configuration effectively prevents over-cracking or excess coke formation by properly regulating the contact between the feed molecules and the zeolites, removing the distillates to the gas phase. Proper selection of inert-gas flow rate, which further regulates the contact time, can further enhance the PE conversion and liquid selectivity. Among the tested commercial zeolites, zeolite beta having the \*BEA topology exhibited excellent acid site strength, ensuring high conversion of PE even at low temperature and an adequate shape selectivity towards aliphatic liquid products. Along with the Al content of zeolites, the crystal size was confirmed as a crucial factor determining the PE conversion and liquid phase selectivity. Reducing the crystal size ensures high liquid selectivity regardless of the Al content by enhancing the chain scission on the external surfaces of zeolites. This work not only highlights the potential for the low-temperature catalytic cracking of PE using zeolite catalysts but also provides insights into other plastic waste chemical recycling technologies in terms of selection of catalysts<sup>47</sup>. All \*BEA-type zeolites presented in this work were synthesized using conventional hydrothermal methods, recipes that are modifications of the previously reported methods in the literature<sup>36,42,43</sup>. Initially, Al sources, OSDA(TEAOH), mineralizers, and water were mixed to achieve a desired gel composition in 40mL PTFE liners. Subsequently, Si sources were added, ensuring complete dispersion and homogenization by subsequent stirring. The general gel composition can be described as 1.0 SiO<sub>2</sub>: x Al: y TEAOH: z (NH<sub>4</sub>F or NaOH): w H<sub>2</sub>O. x determines the Al content, while y, z, and w depend on the different sample series yielding different crystal sizes. Additional aging steps can be added depending on the sample series. The PTFE liners charged with gels were clad in steel autoclaves and transferred to a convection oven preheated to the desired temperature, which could be rotating or static. The progress of crystallization was tracked by analyzing PXRD patterns of aliquots collected every 37 days. Following crystallization, the products were thoroughly rinsed with distilled water and acetone and calcined at 580C for 6h. The resultant \*BEA-type zeolites were then converted into their H-forms through ion exchange with ammonium nitrate (NH<sub>4</sub>NO<sub>3</sub>) and subsequent calcination at 580C for 6h. The details of the preparations of the three series of samples (L-, M-, and S-series), including specified gel compositions, are provided in the Supplementary Information, together with the characterization of the resulting zeolites. Open-batch catalytic cracking process of PE/Polyolefin catalytic cracking was conducted using open-batch reactive distillation setup in a stirring batch reactor (CheMReSys, R-201) with custom modifications to allow an inert gas flow. Initially, 1g of zeolite catalyst and 10g of model feed PE (LDPE, melt index 25g/10min at 190C/2.16kg, average Mw ~204kDa by GPC, Sigma Aldrich) were placed in a 75mL stainless steel liner and sealed within the stirring reactor. The stainless tubing and fitting connected to the reactor were heated to 330C during the operation with heating tapes to minimize condensation and residue within the tubing and fitting. The reaction was performed for 2h at a bulk temperature of 330C with stirring at 200rpm using an impeller-type stirrer. Simultaneously, inert gas (N<sub>2</sub>) flowed at a desired rate. The liquid product was collected via a condensation device connected to a cold constant-temperature circulation column set at 15C, comprising two stages to minimize the process loss. The gaseous product was collected in a gas sampling bag connected to the end of the reactive distillation setup and analyzed using a GC-FID. The details of quantification methods and reactor structure/operation modes are provided in the Supplementary Information. Characterizations Powder X-ray diffraction (XRD) patterns were obtained with a SMARTLAB instrument (Rigaku, Japan). Scanning electron microscopy (SEM) images and elemental compositions of the zeolites were analyzed using a JSM-7800F Prime microscope equipped with an energy-dispersive spectroscopy (EDS) unit, specifically SDD type with active area of 80mm<sup>2</sup>. EDS was standardized using Certified Reference Materials (CRMs) to ensure accuracy by JEOL Ltd. N<sub>2</sub> physisorption (77K) isotherms were measured using a BELSORP MINI X sorption analyzer. Prior to measurements, samples underwent a 3-h degassing step at 300C using a BELPREP VAC II instrument (MicrotracBEL, Japan). Raman spectra of solid samples were recorded with a DXR2xi instrument (Thermo Fisher Scientific, USA). The selectivity distributions of liquid products were determined using a ChroZen gas chromatography-flame ionization detector (GC-FID, Youngin, Korea), and product identification was carried out with a TSQ 3000 Evo gas chromatography-mass spectrometry (GC-MS) system (Thermo Fisher Scientific, USA) based on the NIST library. The data used in this study are available from the corresponding author upon reasonable request. Chang, C.-F. & Rangarajan, S. Machine learning and informatics based elucidation of reaction pathways for upcycling model polyolefin to aromatics. *J. Phys. Chem. A* 127, 29582966 (2023). Article MATH Google Scholar Cressey, D. Bottles, bags, ropes and toothbrushes: the struggle to track ocean plastics. *Nature* 536, 263265 (2016). Article Google Scholar Geyer, R., Jambeck, J. R. & Law, K. L. Production, use, and fate of all plastics ever made. *Sci. Adv.* 3, e1700782 (2017). Article Google Scholar Joshi, C., Browning, S. & Seay, J. Combating plastic waste via Trash to Tank. *Nat. Rev. Earth Environ.* 1, 142142 (2020). Article Google Scholar Alonso, J. A., Aguado, J. & Serrano, D. P. Feedstock recycling of plastic wastes (Royal Society of Chemistry, 1999). Jiang, J. et al. From plastic waste to wealth using chemical recycling: a review. *J. Environ. Chem. Eng.* 10, 106867 (2022). Article MATH Google Scholar Kleme, J. J., Fan, Y. V. & Jiang, P. Plastics: friends or foes? The circularity and plastic waste footprint. *Energy Sources A Recov. Util. Environ. Eff.* 43, 15491565 (2021). Article MATH Google Scholar Wang, Y. et al. Elucidating the structure-performance relationship of typical commercial zeolites in catalytic cracking of low-density polyethylene. *Catal. Today* 405-406, 135143 (2022). Article MATH Google Scholar Ma, W. et al. Characterization of tar evolution during DC thermal plasma steam gasification from biomass and plastic mixtures: parametric optimization via response surface methodology. *Energy Convers. Manage.* 225, 113407 (2020). Article MATH Google Scholar Wang, N. M. et al. Chemical recycling of polyethylene by tandem catalytic conversion to propylene. *JACS* 144, 1852618531 (2022). Article MATH Google Scholar Conk, R. J. et al. Catalytic deconstruction of waste polyethylene with ethylene to form propylene. *Science* 377, 15611566 (2022). Article MATH Google Scholar Aguado, R., Olazar, M., San Jos, M. J., Gaisin, B. & Bilbao, J. Wax formation in the pyrolysis of polyolefins in a conical spouted bed reactor. *Energy Fuels* 16, 14291437 (2002). Article Google Scholar Sharuddin, S. D., Abnisa, F., Wan Daud, W. M. A. & Aroua, M. K. A review on pyrolysis of plastic wastes. *Energy Convers. Manage.* 115, 308326 (2016). Article Google Scholar Pandey, D. S., Katsaros, G., Lindfors, C., Leahy, J. J. & Tassou, S. A. Fast pyrolysis of poultry litter in a bubbling fluidised bed reactor: energy and nutrient recovery. *Sustainability* 11, 2533 (2019). Article Google Scholar Songip, A. R., Masuda, T., Kuwahara, H. & Hashimoto, K. Test to screen catalysts for reforming heavy oil from waste plastics. *Appl. Catal. B* 2, 153164 (1993). Article Google Scholar Ng, S. H., Seoudi, H., Stanciulescu, M. & Sugimoto, Y. Conversion of polyethylene to transportation fuels through pyrolysis and catalytic cracking. *Energy Fuels* 9, 735742 (1995). Article Google Scholar Rorrer, J. E., Troyano-Valls, C., Beckham, G. T. & Romn-Leshkov, Y. Hydrogenolysis of polypropylene and mixed polyolefin plastic waste over Ru/C to produce liquid alkanes. *ACS Sustain. Chem. Eng.* 9, 1166111666 (2021). Article Google Scholar Bin Jumah, A., Anbumuthu, V., Tedstone, A. A. & Garforth, A. A. Catalyzing the hydrocracking of low density polyethylene. *Ind. Eng. Chem. Res.* 58, 2060120609 (2019). Article Google Scholar Liu, S., Kots, P. A., Vance, B. C., Danielson, A. & Vlachos, D. G. Plastic waste to fuels by hydrocracking at mild conditions. *Sci. Adv.* 7, eabf8283 (2021). Article Google Scholar Rorrer, J. E., Beckham, G. T. & Romn-Leshkov, Y. Conversion of polyolefin waste to liquid alkanes with Ru-based catalysts under mild conditions. *JACS Au* 1, 812 (2020). Article Google Scholar Kim, D. et al. Metathesis, molecular redistribution of alkanes, and the chemical upgrading of low-density polyethylene. *Appl. Catal. B* 318, 121873 (2022). Article Google Scholar Ellis, L. D. et al. Tandem heterogeneous catalysis for polyethylene depolymerization via an olefin-intermediate process. *ACS Sustain. Chem. Eng.* 9, 623628 (2021). Article Google Scholar Okonsky, S. T., Krishnan, J. J. & Toraman, H. E. Catalytic co-pyrolysis of LDPE and PET with HZSM-5, H-beta, and HY: experiments and kinetic modelling. *React. Chem. Eng.* 7, 21752191 (2022). Article Google Scholar Figueiredo, A. L. et al. Catalytic cracking of LDPE over nanocrystalline HZSM-5 zeolite prepared by seed-assisted synthesis from an organic-template-free system. *J. Anal. Appl. Pyrolysis* 117, 132140 (2016). Article MATH Google Scholar Uemichi, Y., Kashiwaya, Y., Tsukidate, M., Ayame, A. & Kanoh, H. Product distribution in degradation of polypropylene over silica-alumina and CaX zeolite catalysts. *Bull. Chem. Soc. Jpn.* 56, 27682773 (1983). Article Google Scholar Audisio, G., Bertini, F., Beltrame, P. L. & Carniti, P. Catalytic degradation of polyolefins. *Makromol. Chem. Marcomol. Symp.* 57, 191209 (1992). You, Y. S., Shim, J.-S., Kim, J.-H. & Seo, G. Liquid-phase degradation of polyethylene wax over mordenite catalysts with different Si/Al molar ratios. *Catal. Lett.* 59, 221227 (1999). Article MATH Google Scholar Corma, A., Planells, J., Sanchez-Marin, J. & Tomas, F. The role of different types of acid site in the cracking of alkanes on zeolite catalysts. *J. Catal.* 93, 3037 (1985). Article Google Scholar Kissin, Y. V. Chemical mechanisms of catalytic cracking over solid acidic catalysts: alkanes and alkenes. *Catal. Rev.* 43, 85146 (2001). Article MATH Google Scholar Amin, A. M., Croiset, E. & Epling, W. Review of methane catalytic cracking for hydrogen production. *Int. J. Hydrogen Energy* 36, 29042935 (2011). Article MATH Google Scholar Lin, Q.-F. et al. A stable aluminosilicate zeolite with intersecting three-dimensional extra-large pores. *Science* 374, 16051608 (2021). Article MATH Google Scholar Gaca, P., Drzewiecka, M., Kaleta, W., Kozubek, H. & Nowiska, K. Catalytic degradation of polyethylene over mesoporous molecular Sieve MCM-41 modified with heteropoly compounds. *Pol. J. Environ. Stud.* 17, 2531 (2008). Serrano, D. P., Aguado, J. & Escola, J. M. Catalytic cracking of a polyolefin mixture over different acid solid catalysts. *Ind. Eng. Chem. Res.* 39, 11771184 (2000). Article MATH Google Scholar Park, J. W., Kim, J.-H. & Seo, G. The effect of pore shape on the catalytic performance of zeolites in the liquid-phase degradation of HDPE. *Polym. Degrad. Stab.* 76, 495501 (2002). Article MATH Google Scholar Cambor, M., Mifud, A. & Prez-Pariente, J. Influence of the synthesis conditions on the crystallization of zeolite Beta. *Zeolites* 11, 792797 (1991). Article Google Scholar Mintova, S. et al. Variation of the Si/Al ratio in nanosized zeolite Beta crystals. *Microporous Mesoporous Mater.* 90, 237245 (2006). Article Google Scholar Caldeira, V. P. et al. Properties of hierarchical Beta zeolites prepared from protozeolitic nanounits for the catalytic cracking of high density polyethylene. *Appl. Catal. A* 531, 187196 (2017). Article MATH Google Scholar Peral, A. et al. Bidimensional ZSM-5 zeolites probed as catalysts for polyethylene cracking. *Catal. Sci. Technol.* 6, 27542765 (2016). Article MATH Google Scholar Hittinger, J. P. & Shantz, D. F. Systematic study of low temperature cracking of low-density polyethylene with ZSM-5. *Microporous Mesoporous Mater.* 343, 112170 (2022). Article MATH Google Scholar Wang, Y.-Y. et al. Catalytic hydrogenolysis of polyethylene under reactive separation. *ACS Catal.* 14, 20842094 (2024). Article MATH Google Scholar Sandoval-Daz, L.-E., Gonzlez-Amaya, J.-A. & Trujillo, C.-A. General aspects of zeolite acidity characterization. *Microporous Mesoporous Mater.* 215, 229243 (2015). Article MATH Google Scholar Jon, H., Lu, B., Oumi, Y., Itabashi, K. & Sano, T. Synthesis and thermal stability of beta zeolite using ammonium fluoride. *Microporous Mesoporous Mater.* 89, 8895 (2006). Article Google Scholar Xie, B. et al. Organotemplate-free and fast route for synthesizing beta zeolite. *Chem. Mater.* 20, 45334535 (2008). Article MATH Google Scholar Xia, Q.-H., Shen, S.-C., Song, J., Kawi, S. & Hidajat, K. Structure, morphology, and catalytic activity of zeolites synthesized in a fluoride medium for asymmetric hydrogenation. *J. Catal.* 219, 7484 (2003). Article Google Scholar Lpez, A., de Marco, I., Caballero, B. M., Adrados, A. & Laresgoiti, M. F. Deactivation and regeneration of ZSM-5 zeolite in catalytic pyrolysis of plastic wastes. *Waste Manage.* 31, 18521858 (2011). Article Google Scholar Williams, P. T. & Brindle, A. J. Catalytic pyrolysis of tyres: influence of catalyst temperature. *Fuel* 81, 24252434 (2002). Article MATH Google Scholar Rorrer, J. E. et al. Role of Bifunctional Ru/acid catalysts in the selective hydrocracking of polyethylene and polypropylene waste to liquid hydrocarbons. *ACS Catal.* 12, 1396913979 (2022). Article Google Scholar Download references This research was supported by Korea Institute of Industrial Technology (KITECH) through the Korea Environmental Industry & Technology Institute (KEITI) funded by the Ministry of Environment (ARQ202209004001). The authors declare no competing financial interest. Communications Engineering thanks Makenna Pennel and the other, anonymous, reviewers for their contribution to the peer review of this work. Peer review reports are available.